New isotope ^{264}Sg and decay properties of $^{262\text{-}264}$Sg

K. E. Gregorich,[1] J. M. Gates,[1,2] Ch. E. Düllmann,[3] R. Sudowe,[1] S. L. Nelson,[1,2] M. A. Garcia,[1,2] I. Dragojević,[1,2] C. M. Folden III,[4] S. H. Neumann,[5] D. C. Hoffman,[1,2] H. Nitsche[1,2]

[1]*Nuclear Science Division, Lawrence Berkeley National Laboratory, Berkeley, California 94720*

[2]*Department of Chemistry, University of California, Berkeley, California 94720*

[3]*Gesellschaft für Schwerionenforschung, D-64291 Darmstadt, Germany*

[4]*National Superconducting Cyclotron Laboratory, Michigan State U., East Lansing, Michigan 48824*

[5]*Dept. of Applied Sciences and Technology, Aachen U. of Applied Sciences, D-52428 Jülich, Germany*

(20 June 2006)

New isotope, ^{264}Sg, was identified using the ^{38}U(^{30}Si,xn)$^{268\text{-}x}$Sg reaction and excitation functions for $^{262\text{-}264}$Sg were measured. ^{264}Sg decays by spontaneous fission with a half life of 37^{+27}_{-11} ms. The spontaneous fission branch for 0.9-s ^{263}Sg was measured for the first time and found to be (13±8)%. ^{262}Sg decays by spontaneous fission with a 15^{+5}_{-3} ms half-life. Spontaneous fission partial half-life systematics are evaluated for even-even Sg isotopes from ^{258}Sg through ^{266}Sg, spanning the transition region between the N=152, Z=100 and N=162, Z=108 deformed shells.

PACS Number(s): 25.60Pj, 25.85Ca, 27.90+b

Reactions between actinide targets and low-Z projectiles from C to Al have been used to produce heavy element isotopes up to Z=108. Surprisingly large superheavy element formation cross sections have recently been reported in hot fusion reactions between ^{48}Ca beams and actinide targets [1-3]. Understanding these superheavy element formation cross sections is hindered by the dearth of reports of hot fusion reactions between actinide targets and projectiles between ^{26}Mg and ^{48}Ca.

We have studied the production of Sg (Z=106) isotopes via the ^{238}U(^{30}Si,xn)$^{268-x}$Sg hot fusion reaction. In addition to providing data for understanding hot fusion reactions, these experiments allow the study of the decay properties of three Sg isotopes. ^{262}Sg, a short-lived spontaneous fission (SF) activity, has been produced as the decay product of ^{270}Ds [4], only 8 atoms have been observed. There are indications for isomerism in the decay of ^{263}Sg [5-10], and no experiments to date have been sensitive to SF decay of the 0.9-s isomer. ^{264}Sg is unknown. Measurement of the SF properties of these isotopes, in the transition region between deformed neutron shells at N=152 and N=162, provides important information in the understanding of SF half-life systematics.

The LBNL 88-Inch Cyclotron accelerated beams of ^{30}Si to energies of 5.2-6.0 MeV/A. At the entrance to the Berkeley Gas-filled Separator (BGS), the beam passed through a 45 μg/cm^2 carbon entrance window which separates the beamline vacuum from the 66-Pa He gas inside the BGS. $^{238}UF_4$ targets were prepared by evaporation of UF_4 onto 0.58 mg/cm^2 arc-shaped Al backing foils. Nine of the UF_4 target segments were arranged on the periphery of a 35-cm diameter target wheel located approximately 1 cm downstream of the carbon entrance window. To prevent local overheating of the targets, the target wheel was rotated at ~ 500 Hz. The energy

thickness of the UF_4 target layer was approximately 2.4 MeV [11]. Relative beam energies in the targets were monitored with two Si *p-i-n* diode "monitor detectors," mounted at ±27-degrees from the beam axis, that detected Rutherford-scattered projectiles. An analysis of the pulse-heights from the various ^{30}Si beam energies indicated in-target beam energy ranges of 148.7±2.2, 155.1±1.2, 165.1±2.2, and 173.1±1.2 MeV. This analysis provides relative beam energies accurate to ~0.3%, while a systematic error of ~1% remains for the absolute energies. Compound nucleus excitation energies were calculated using these beam energy ranges and experimental mass defects [12] for ^{30}Si and ^{238}U and target, together with Thomas-Fermi mass defects [13,14] for the compound nuclei. The resulting ranges of compound nucleus excitation energies within the targets were 39.3±2.0, 44.8±1.1, 53.7±2.0, and 60.8±1.1 MeV. The rate of Rutherford-scattered projectiles in the monitor detectors was used to continuously monitor the product of beam intensity and target thickness. Beam intensities ranged from 0.6-1.2 particle-μA.

Sg compound nuclei evaporation residues (EVRs) are formed with the momentum of the projectile and recoil from the target. The BGS separates them from the beam and other reaction products by their differing magnetic rigidities in He gas. Magnetic rigidities for the Sg EVRs were estimated as in previous work [15]. The efficiency, eff, for collecting Sg EVRs at the BGS focal plane was estimated using a Monte Carlo simulation of the EVR trajectories in the BGS, as described earlier [15, 16]. These simulations resulted in $eff = 0.30 \pm 0.06$. Details of the Si-strip detector array and data acquisition systems are as reported earlier [10, 15]. However, because of the short range expected for the Sg EVRs, no multiwire proportional counter was used.

During the irradiations, the rate of "EVR-like events" ($5.0 < E(MeV) < 14.0$, anticoincident with upstream or punchthrough detectors) was 1.7 Hz. The rate of "Sg-like events" ($8.0 < E(MeV) < 10.5$, focal plane only or reconstructed from focal plane + upstream detector, anticoincident with punchthrough detector) was 0.04 Hz. ^{263}Sg was identified by detection of time and position correlated event chains corresponding to EVR implantation followed by the α-decay of ^{263}Sg and ^{259}Rf (and possibly ^{255}No). To minimize the contribution of random correlation of unrelated events, a two-stage fast beam-shutoff scheme was employed. Upon detection of an EVR-like event followed by a position- and time-correlated (within 2 σ and 4 s) ^{263}Sg-like event, the beam was switched off for 12 s to perform a background-free search for "Rf-like events" ($7.5 < E(MeV) < 9.5$, focal plane only or reconstructed from focal plane + upstream detector, anticoincident with punchthrough detector). If a position-correlated (within 2σ) daughter-like event was detected during the beamoff interval, the shutoff time was extended for 900 s to allow a background-free search for the α-decay of the longer-lived ^{255}No granddaughter. Slightly wider beam-shutoff gates were used during portions of the experiments.

The spectrum of all focal plane events with $0.5<E(MeV)<20$ in the high-gain ADCs (anticoincident with punchthrough detector) is presented in Fig. 1. The small alpha peaks near 6.8 MeV are due to ^{181}Ta(^{30}Si,xn)$^{211-x}$Fr reactions occurring in the Ta beamstop. A small fraction of these Fr reaction products scatters out of the beamstop and obtains trajectories reaching the BGS focal plane. The spectrum of all focal plane events with E>19 MeV in the low-gain ADCs is also presented in Fig. 1. The broad peak near 33 MeV is due to elastically scattered ^{238}U. The Fig. 1 inset spectrum shows all events

with 5<E(MeV)<10 during the beamoff intervals. All event chains assigned to the formation and decay of Sg isotopes are presented in Table I. The magnetic rigidity of the Sg EVRs was 2.36±0.06 T·m

Five SF events assigned to new isotope ^{264}Sg, produced by the ^{238}U(^{30}Si,4n)^{264}Sg reaction, were observed at the lowest ^{30}Si energy (events 1-5 in Table I). Assignment of these SF events to the 4n exit channel is supported mainly by the fact that this reaction energy is below threshold for the 6n exit channel, and only 4.7 MeV above the 5n exit channel threshold. The half-life resulting from these five SF decay lifetimes is 37^{+27}_{-11} ms. α-decay of ^{264}Sg (followed by the SF decay of 20-ms ^{260}Rf) was not observed, resulting in an α-decay branch upper limit of <36%. The corresponding partial half-life for α-decay is >100 ms. This is consistent with the expected partial α-decay half-life of 0.8 s calculated with the expected 9.21-MeV Q-value for α decay of ^{264}Sg [12] and the Hatsukawa α-decay systematics [17]. The ^{238}U(^{30}Si,4n)^{264}Sg cross section is 9^{+6}_{-4} pb.

^{263}Sg is produced by the ^{238}U(^{30}Si,5n)^{263}Sg reaction at the three highest reaction energies. Seven events are assigned to the α-decay of ^{263}Sg (events 6, 8-13 in Table I) and three events are assigned to the SF decay of ^{263}Sg (events 7, 14, and 24 in Table I). Assignment of these three EVR-SF events to the decay of ^{263}Sg rather than the neighboring even-even Sg isotopes is based on the relatively long lifetimes of >159 ms. The corresponding SF branch in ^{263}Sg is (13±8)%. The half-life calculated from all 10 events assigned to the decay of ^{263}Sg is $0.82^{+0.37}_{-0.19}$ s, which compares well with the ~1.0-s half-life reported earlier [5, 6]. The half-life measured for the ^{259}Rf daughter is $1.9^{+1.3}_{-0.5}$ s, and that for the ^{255}No granddaughter is $3.0^{+2.3}_{-0.9}$ m. These values are consistent with

accepted values [18] of 2.8 s and 3.1 min, respectively. It should be noted that direct production of ^{263}Sg favors population of the 0.9-s ^{263}Sg isomer, and that this is the first measurement of its SF branch.

Fifteen SF events assigned to the SF decay of ^{262}Sg, produced in the ^{238}U(^{30}Si,6n)^{262}Sg reaction were observed (events 15-23, and 25-30 in Table I) at the two highest reaction energies. Lifetimes less than 51 ms separate these EVR-SF correlations from SF of 0.9-s ^{263}Sg. The half-life resulting from these fifteen decay lifetimes is 15^{+5}_{-3} ms, which is longer than the previously reported value of $6.9^{+3.8}_{-1.8}$ ms [4]. α-decay of ^{262}Sg (followed by the SF decay of 12-ms ^{258}Rf) was not observed, resulting in an α-decay branch upper limit of <16%. The corresponding partial half-life for α-decay is >95 ms. This value is similar to the estimate of 60 ms calculated with a Q-value for α-decay of 9.60 MeV [12], and the Hatsukawa α-decay systematics [17].

During the entire experiment, there were 29 events with focal plane signals above 101 MeV. 23 of these have been assigned to SF of Sg isotopes. The actual rate of random EVR-like signals preceding the 23 SF events assigned to decay of Sg isotopes within a vertical window of ± 1.3 mm (the largest EVR-SF position difference in Table I) was 3×10^{-3} Hz. With a total of 29 SF-like events, the number of random EVR-SF correlations expected with SF lifetimes less than 100 ms is 9×10^{-3}. Thus it is unlikely that any of the 20 EVR-SF correlations assigned to the decay of ^{264}Sg or ^{262}Sg are random correlations of unrelated events. During the 3.6-s time intervals (four times the 0.9-s ^{263}Sg half-life) preceding the remaining nine SF-like events, ~0.1 random EVR-SF correlations are expected. Thus it is also unlikely that any of the EVR-SF correlations assigned to the decay of ^{263}Sg are of random origin.

During the entire experiment, there were a total of 2782 first-level beam shutoffs due to potential EVR - ^{263}Sg correlations, and 6 second-level beam shutoffs due to potential EVR - ^{263}Sg - ^{259}Rf correlations. A total of 16 ^{259}Rf-like events with $8.7 < E(MeV) < 9.0$ were recorded during the beamoff intervals. Of these, 7 are strip- and position-correlated to the EVR-α sequence initiating the beam shutoff, leading to the conclusion of a negligible contribution of random correlations in the search for ^{263}Sg-^{259}Rf (-^{255}No) decay chains.

Excitation functions for 4n, 5n, and 6n exit channels from the ^{238}U(^{30}Si,xn)$^{268-x}$Sg reaction, according to the assignments in Table I, are plotted in Fig. 2. Vertical error bars represent uncertainties due to counting statistics only. Horizontal bars show the range of compound nucleus excitation energies in the targets. The ^{238}U(^{30}Si,5n)^{263}Sg reaction has the largest maximum cross section, with the centroid at approximately 50 MeV, as expected for the 5n exit channel. The 6n exit channel, leading to SF of ^{262}Sg has a peak cross section approximately a factor of 2.5 smaller at a centroid energy of about 57 MeV. The 37-ms SF events assigned to the formation and decay of ^{264}Sg occur at the 39.3-MeV, which is clearly separated from the 15-ms SF assigned to ^{262}Sg.

Systematics of partial SF half-lives for the even-even Sg isotopes are displayed in Fig. 3. This plot contains a revised $2.8^{+0.8}_{-0.5}$ ms half-life for ^{258}Sg [19, 20], A partial SF half-life calculated from accepted values for ^{260}Sg [18], a revised half-life for ^{262}Sg (this work), the SF half-life for new isotope ^{264}Sg (this work), and a recent result for the ^{266}Sg SF half-life [21]. At $96 \leq Z \leq 102$, partial SF half-lives are strongly peaked at N=152. This influence of the deformed shells at Z=100 and N=152 [22] is absent at Z=106.

However, the relatively long SF half-life for ^{266}Sg [21] may indicate enhanced stability due to deformed shells at Z=108 and N=162.

We gratefully acknowledge the operations staff of the 88-Inch Cyclotron for providing the intense beams of ^{30}Si. ^{238}U targets were produced in collaboration with Walter Loveland at Oregon State University. Financial support was provided by the Office of High Energy and Nuclear Physics, Nuclear Physics Division of the U.S. Department of Energy, under contract DE-AC03-76SF000988.

---

[1] Yu. Ts. Oganessian *et al.*, Phys. Rev. C **69**, 021601(R) (2004).
[2] Yu. Ts. Oganessian *et al.*, Phys. Rev. C **69**, 054607 (2004).
[3] Yu. Ts. Oganessian *et al.*, Phys. Rev. C **70**, 064609 (2004).
[4] S. Hofmann *et al.*, Eur. Phys. J. A **10**, 5 (2001).
[5] A. Ghiorso *et al.*, Phys. Rev. Lett. **33**, 1490 (1974).
[6] K. E. Gregorich *et al*., Phys. Rev. Lett. **72**, 1423 (1994).
[7] S. Hofmann, Rep. Prog. Phys. **61**, 639 (1998).
[8] T. N. Ginter *et al.*, Phys. Rev. C **67**, 064609 (2003).
[9] K. Morita *et al.*, Eur. Phys. J. A **21**, 257 (2004).
[10] C. M. Folden III *et al.*, Phys. Rev. Lett. **93**, 212702 (2004).
[11] J. F. Ziegler, Nucl. Instrum. Methods Phys. Res. B **219-220**, 1027 (2004).
[12] G. Audi, A. H. Wapstra, and C. Thibault, Nucl. Phys. **A729**, 337 (2003).
[13] W. D. Myers and W. J. Swiatecki, Nucl. Phys. **A601**, 141 (1996).
[14] W. D. Myers and W. J. Swiatecki, Lawrence Berkeley National Laboratory Report; LBNL-36803 (1994). http://ie.lbl.gov/txt/ms.txt
[15] K. E. Gregorich *et al.*, Phys. Rev. C **72**, 014605 (2005).
[16] K. E. Gregorich *et al.*, Eur. Phys. J. A **18**, 633 (2003).
[17] Y. Hatsukawa, H. Nakahara, and D. C. Hoffman, Phys. Rev. C **42**, 674 (1990).
[18] G. Audi, O. Bersillon, J. Blachot, and A. H. Wapstra, Nucl. Phys. **A729**, 3 (2003).
[19] F. P. Heβberger *et al.*, Z. Phys. A **359**, 415 (1997).
[20] J. B. Patin, Lawrence Berkeley National Laboratory Report, LBNL-49593 (2002).
[21] A. Türler, private communication.
[22] D. C. Hoffman and M. R. Lane, Radiochim. Acta **70/71**, 135 (1995).

Table I. Observed Sg decay chains. For reconstructed energies, the energies recorded in the focal plane and upstream detectors, respectively, are listed in parentheses. SF energies are shown in boldface.

E* (MeV)	event #	strip	E_{EVR} (MeV)	position (mm)	decay energy (MeV)	position (mm)	lifetime	^{A}Z
39.3	1	16	7.84	25.3±0.4	**234 (175+59)**	24.8±1.5	76.61 ms	^{264}Sg
	2	42	8.08	-15.6±0.3	**120**	-14.4±1.5	20.01 ms	^{264}Sg
	3	28	6.09	-18.0±0.5	**159 (127+32)**	-17.7±1.5	33.91 ms	^{264}Sg
	4	21	6.34	29.2±0.4	**138**	28.4±1.5	40.27 ms	^{264}Sg
	5	3	6.36	-22.1±0.4	**134**	-22.4±1.5	96.12 ms	^{264}Sg
44.8	6	11	8.90	-25.6±0.3	9.29	-25.1±0.3	0.704 s	^{263}Sg
					8.85	-25.5±0.3	1.324 s	^{259}Rf [a]
					7.85	-25.3±0.4	266.1 s	^{255}No[a]
	7	8	10.20	-11.6±0.3	**174 (151+23)**	-11.6±1.5	0.246 s	^{263}Sg
53.7	8	30	6.72	-20.3±0.4	9.01	-19.8±0.3	2.119 s	^{263}Sg
					8.87 (0.65+8.22)	<0.0 [b]	3.017 s	^{259}Rf [a]
	9	8	7.73	10.0±0.4	9.23 (0.72+8.51)	3.7±0.3	1.755 s	^{263}Sg
					8.79 (1.38+7.41)	9.0±0.3	4.354 s	^{259}Rf [a]
					8.15	9.0±0.3	16.47 s	^{255}No[a]
	10	17	7.40	16.2±0.4	9.10	15.9±0.3	0.814 s	^{263}Sg
					8.87	16.2±0.3	4.988 s	^{259}Rf [a]
					8.00	15.5±0.4	104.5 s	^{255}No[a]
	11	9	10.83	3.2±0.3	8.87 (1.27+7.60)	-1.6±0.3	0.861 s	^{263}Sg
					8.97 (1.00+7.98)	-1.1±0.3	3.844 s	^{259}Rf [a]
					7.74	3.1±0.4	659.1 s	^{255}No[a]
	12	7	7.13	-18.3±0.4	9.06	-18.2±0.3	2.628 s	^{263}Sg
					8.90	-18.2±0.3	1.053 s	^{259}Rf [a]
	13	22	8.46	-8.0±0.3	9.06	-8.0±0.3	0.994 s	^{263}Sg
					8.80	-8.3±0.3	0.549 s	^{259}Rf [a]
					7.99	-8.0±0.4	246.1 s	^{255}No[a]
	14	38	7.37	-11.3±0.4	**167 (132+35)**	-10.8±1.5	159.8 ms	^{263}Sg
	15	34	5.05	-15.1±0.6	**138**	-14.1±1.5	3.433 ms	^{262}Sg
	16	12	11.1	-12.9±0.3	**173 (152+21)**	-12.6±1.5	16.18 ms	^{262}Sg
	17	1	9.92	20.9±0.3	**108**	21.0±1.5	11.13 ms	^{262}Sg
	18	6	8.50	-11.8±0.3	**169 (158+11)**	-11.7±1.5	46.88 ms	^{262}Sg
	19	12	7.13	20.2±0.4	**190**	20.3±1.5	32.76 ms	^{262}Sg
	20	7	8.26	-7.0±0.3	**191**	-6.6±1.5	5.364 ms	^{262}Sg
	21	29	10.03	-28.9±0.3	**176**	-28.0±1.5	22.40 ms	^{262}Sg
	22	33	9.67	25.3±0.3	**192**	24.9±1.5	13.80 ms	^{262}Sg
	23	15	9.04	-20.1±0.3	**179**	-19.7±1.5	16.30 ms	^{262}Sg
60.8	24	18	8.47	8.3±0.3	**173 (139+34)**	8.4±1.5	1.529 s	^{263}Sg
	25	19	8.78	9.5±0.3	**147 (116+31)**	10.2±1.5	50.72 ms	^{262}Sg
	26	11	9.36	-12.8±0.3	**199 (167+32)**	-12.8±1.5	5.540 ms	^{262}Sg
	27	38	9.59	10.9±0.3	**175**	11.1±1.5	8.438 ms	^{262}Sg
	28	31	9.73	-4.1±0.3	**204**	-5.4±1.5	43.92 ms	^{262}Sg
	29	26	12.06	24.8±0.2	**175 (168+7)**	24.8±1.5	19.64 ms	^{262}Sg
	30	12	10.07	-13.5±0.3	**174 (127+47)**	-13.0±1.5	20.30 ms	^{262}Sg

[a] decay detected with beam switched off

[b] focal plane signal recorded from bottom of strip only, signal from top was below threshold

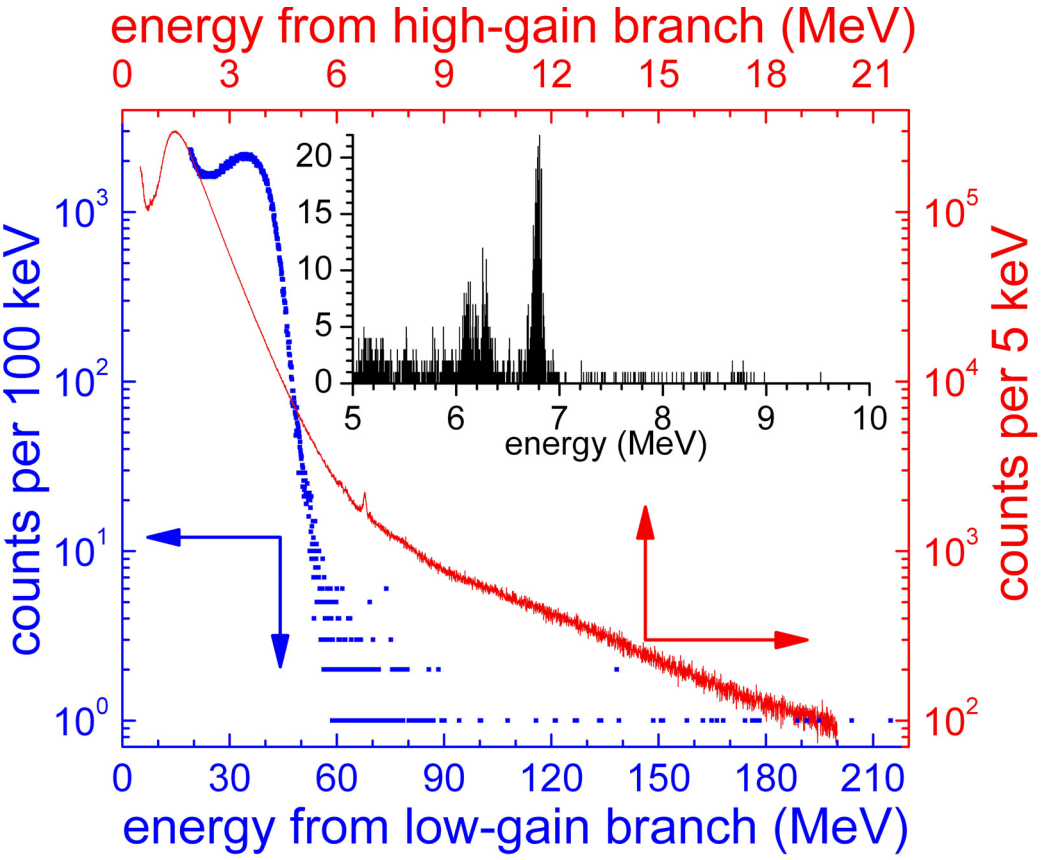

Figure 1. (Color online) Particle spectra recorded in the focal plane detector. The solid line shows events from the high-gain spectra (top and right axes). Points show the low-gain spectra (bottom and left axes). The inset spectrum shows all events with 5<E(MeV)<10 occurring during the beamoff intervals.

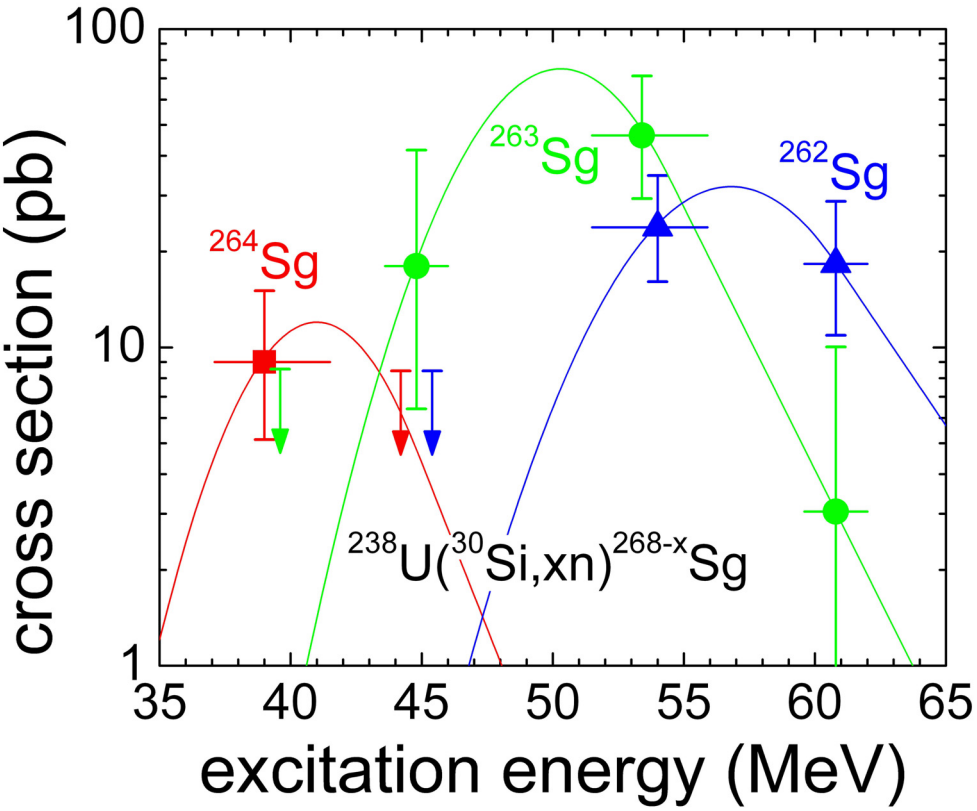

Figure 2. (Color online) Excitation function for the 4n, 5n, and 6n exit channels from the $^{238}U(^{30}Si,xn)^{268-x}Sg$ reaction. Lines are drawn to guide the eye.

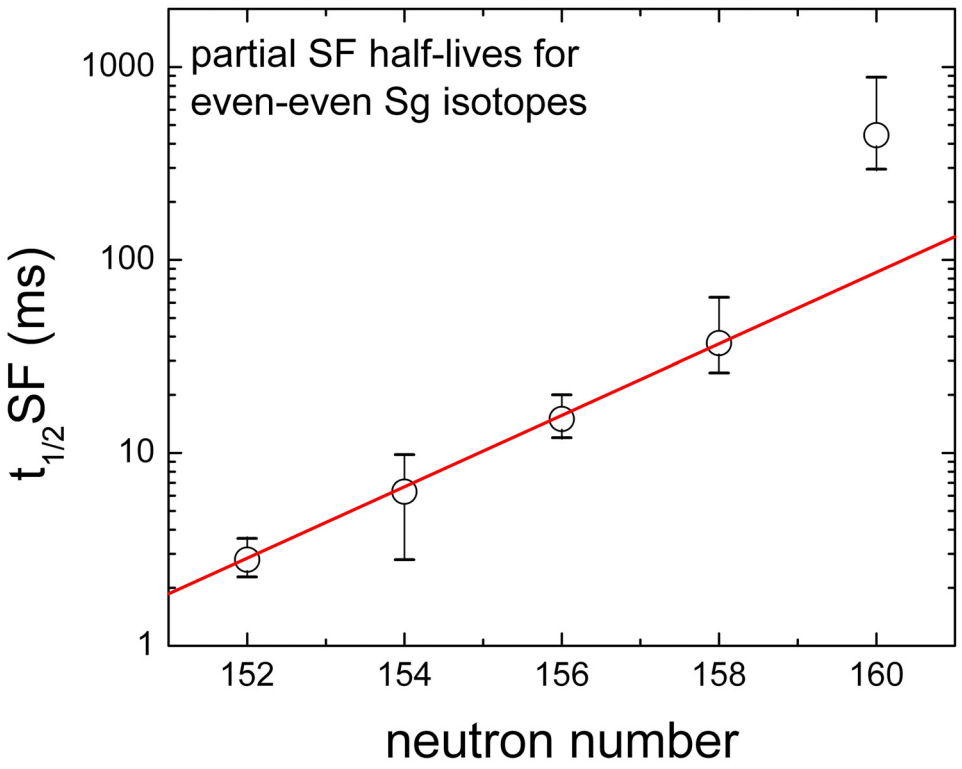

Figure 3. (Color online) Partial spontaneous fission half-lives for even-even Sg isotopes. The line is drawn to guide the eye.